Biotecnia
Journal of biological and health sciences
http://biotecnia.unison.mx
Universidad de Sonora
ISSN: 1665-1456

Original Article

Activity of starch biosynthetic enzymes and their association with endosperm modification in quality protein maize

Actividad de enzimas de biosíntesis de almidón y su asociación con la modificación del endospermo en maíz de calidad proteínica

David G. González-Núñez[1], Jesús C. Grimaldi-Olivas[1], Karen V. Pineda-Hidalgo[1], Héctor S. López-Moreno[1], María E. Báez-Flores[1], Edith Agama-Acevedo[2], Nancy Y. Salazar-Salas[1]* and José A. Lopez-Valenzuela[1]*

[1] Facultad de Ciencias Químico-Biológicas, Universidad Autónoma de Sinaloa, Culiacán, Sinaloa, México, C.P. 80010.
[2] Centro de Desarrollo de Productos Bióticos, Instituto Politécnico Nacional, Yautepec, Morelos, México, C.P. 62731.

ABSTRACT

The formation of vitreous endosperm in quality protein maize (QPM) is associated with changes in the composition and structure of starch granules, but little is known about the role of alterations in the structure and activity of the main starch biosynthetic enzymes. Developing endosperms from K0326Y-QPM, W64A*o2*, and derived recombinant inbred lines were used to analyze the activity of ADP-glucose pyrophosphorylase (AGPase), granule-bound starch synthase (GBSS), starch-branching enzyme (SBE) and pullulanase (PULL). GBSS activity correlated positively with kernel vitreousness and the opposite was observed for SBE. SBEIIb enzymes from K0326Y-QPM and W64A*o2* differed in five amino acids. Three amino acid changes appear to affect the SBEIIb catalytic site, which may be responsible for the lower activity and amylopectin content in vitreous lines. However, recombinant SBEIIb enzymes produced in *Escherichia coli* showed similar activities. The results suggest that endosperm modification in QPM is associated with changes in the activity of starch biosynthetic enzymes, which affect the starch composition, physicochemical and structural properties during endosperm development. The higher GBSS activity and the lower SBE activity produce starch granules with more amylose and amorphous regions, favoring the compaction between these structures, contributing to the vitreous phenotype in QPM.

Keywords: quality protein maize; vitreous endosperm; starch biosynthesis.

RESUMEN

La formación del endospermo vítreo en maíz de calidad proteínica (QPM) está asociado con cambios en la composición y estructura de gránulos de almidón, pero se conoce poco acerca del papel de alteraciones en la estructura y actividad de las principales enzimas biosintéticas. Endospermos en desarrollo de K0326Y-QPM, W64A*o2* y líneas recombinantes puras derivadas se utilizaron para analizar la actividad de ADP-glucosa pirofosforilasa (AGPasa), almidón sintasa unida al gránulo (GBSS), enzima ramificadora de almidón (SBE) y pululanasa (PULL). La actividad de GBSS correlacionó positivamente con la vitrosidad del grano y lo opuesto se observó para SBE. Enzimas SBEIIb de K0326Y-QPM y W64A*o2* difirieron en cinco aminoácidos. Tres cambios de aminoácidos parecen afectar el sitio catalítico de SBEIIb, lo cual podría ser responsable de la menor actividad y contenido de amilopectina en líneas vítreas. Sin embargo, enzimas SBEIIb recombinantes producidas en *Escherichia coli* mostraron actividades similares. Los resultados sugieren que la modificación del endospermo en QPM está asociada con cambios en la actividad de enzimas de síntesis de almidón, lo cual afecta la composición, propiedades fisicoquímicas y estructurales del almidón durante el desarrollo del endospermo. La mayor actividad de GBSS y menor actividad de SBE produce gránulos de almidón con más amilosa y regiones amorfas, favoreciendo una mayor compactación entre estas estructuras, contribuyendo al fenotipo vítreo en QPM.

Palabras clave: maíz de calidad proteínica; endospermo vítreo; biosíntesis de almidón

INTRODUCTION

Maize (*Zea mays* L.) is the most important cereal crop worldwide and plays a crucial role as staple food in developing countries from Africa, Asia and Latin America (FAOSTAT, 2024). However, the quality of maize proteins is low because they are deficient in lysine and tryptophan. The *opaque2* (*o2*) mutation increases the content of these essential amino acids and improves the protein quality (Mertz *et al.*, 1964), but it has a poor agronomic performance and postharvest issues due to a soft endosperm. Plant breeders developed *o2* mutants with hard endosperm known as Quality Protein Maize (QPM) by recurrent backcrossing (Maqbool *et al.*, 2021). This lengthy and laborious strategy required the simultaneous selection of vitreous kernels and enhanced levels of essential amino acids. The use of molecular markers has accelerated QPM breeding, but this process could be more efficient if the mechanisms involved in the formation of the vitreous phenotype are understood. The storage 27-kDa γ-zein protein plays an essential role because its elimination disrupts the endosperm modification, whereas the enhanced accumulation of this protein favors the formation of protein bodies and their compaction between starch granules (Wu *et al.*, 2010). Other mechanisms have been proposed based on genetic and biochemical studies (Gonzalez-Nuñez *et al.*, 2023).

*Author for correspondence: Nancy Y. Salazar-Salas and José A. Lopez-Valenzuela
e-mail: nancy.salazar@uas.edu.mx; jalopezvla@uas.edu.mx
Received: August 16, 2024
Accepted: January 27, 2025
Published: February 28, 2025

DOI: 10.18633/biotecnia.v27.2421

Table 1. Primers used to sequence the *Ae1* gene.
Table 1. Iniciadores utilizados para secuenciar el gen *Ae1*.

Name	Sequence	Annealing temperature (°C)	Start	End	Product Size
Ae1-F1	GTAGCCCTGCAGTCA	52	1	644	644
Ae1-R644	CCCATTCTCGATATGTGATAC				
Ae1-F571	GGAAGCCTTCTCCCGTAGTTA	58	571	1106	536
Ae1-R1106	ATGAGTGCTCTTGGATTGCCA				
Ae1-981F	AGCCCGGAACCGAAGATAAA	58	981	1649	669
Ae1-1649R	ACCTACCCCACCATCGTGAA				
Ae1-1627F	CTGTTCACGATGGTGGGGTA	58	1627	2403	777
Ae1-2403R	TATCATGCGAACAGTCGGCG				
Ae1-2024F	CCAAGAGGTCCGCAAAGACT	58	2024	2743	720
Ae1-2743R	CAAACAATCAGCCATCAAGCA				

F: Forward; R: Reverse.
F: Directo; R: Inverso

Genetic mapping using microsatellites and recombinant inbred lines (RILs) from the cross between W64A*o2* and K0326Y-QPM, revealed three quantitative trait loci (QTL) on chromosomes 1, 7, and 9 associated with vitreousness (Holding *et al.*, 2011). The same QTLs were identified in an F2 population derived from the same cross using bulked segregant analysis (BSA) with next generation sequencing (Li *et al.*, 2020). The locus on chromosome 7 corresponded to the 27-kDa γ-zein, whereas the locus on chromosome 9 was close to starch biosynthesis genes and *Pfpa*, which encodes the α-regulatory subunit of pyrophosphate-dependent fructose-6-phosphate 1-phosphotransferase. Linkage mapping of starch physicochemical properties using the same RILs from the cross between W64A*o2* and K0326Y-QPM, identified three QTLs on chromosomes 4, 5, and 9; they were close to the starch biosynthesis genes *Brittle-2* (*Bt2*), *Amylose extender-1* (*Ae1*), and *Waxy-1* (*Wx1*), respectively (Vega-Alvarez *et al.*, 2022). These results agree with previous biochemical studies suggesting that endosperm modification in QPM, is also associated with the synthesis of starch containing a higher proportion of amylose and short-intermediate amylopectin chain branches, which favors the compaction of starch granules and their interaction with protein bodies (Salazar-Salas *et al.*, 2014). The starch biosynthetic enzymes pullulanase and starch synthase III were proposed as important factors in the formation of the vitreous phenotype (Wu *et al.*, 2015). However, little is known about the possible role of alterations in structure and activity of key starch biosynthetic enzymes, such as the branching enzyme in the modification of the *o2* endosperm.

The aim of the present study was to evaluate the activity of starch biosynthesis enzymes and its association with endosperm modification in quality protein maize.

MATERIAL AND METHODS

Materials

The inbred lines K0436Y-QPM (vitreous) and W64A*o2* (opaque), and six F8 recombinant lines (RIL) derived from their cross were used. The selected RILs were contrasting in vitreousness and the genotype of markers flanking QTLs previously identified for endosperm modification (Holding *et al.*, 2011); three vitreous RILs were homozygous for the K0326Y-QPM allele and three opaque RILs were homozygous for the W64A*o2* allele. The materials were grown in the experimental field of the Faculty of Agronomy, Autonomous University of Sinaloa, Culiacan, Sinaloa, México in the Winter-Spring season of 2019-2020. Developing kernels were harvested 28 days after pollination (DAP), frozen in liquid nitrogen and stored at -70 °C until use.

Starch composition

Developing endosperms (28 DAP) were lyophilized and ground into flour to determine total starch content with the STA20 kit (Sigma Aldrich, St. Louis MO, USA). Amylose content was determined from starch using the methodology of ISO 6647-1:2020 (ISO, 2020). Amylopectin content was obtained by difference.

Isolation of starch granules

Starch granules were isolated from developing kernels according to Vega-Alvarez *et al.* (2022). Kernels were soaked in a solution of sodium metabisulfite 0.3 % (w/v) and lactic acid 85 % (v/v) pH 3.8, for 48 h at 50 °C. The germ and the pedicel were removed, and the endosperms were macerated with a mortar and pestle using starch extraction buffer [50 mmol/L Tris-HCl, pH 7, 100 mL/L glycerol, 10 mmol/L EDTA, 1.25 mmol/L DTT] at 4 °C, then passed through a 100 µm filter and centrifuged at 13,000 *g* for 15 min. The starch obtained was washed twice with extraction buffer, 950 mL/L ethanol, and cold acetone, then dried for 12 h at room temperature.

Starch thermal properties

About 2.2 mg of starch were weighed in a hermetic pan and mixed with 7 µL of deionized water. The mixture was equilibrated for 1 h and the pan was sealed for analysis with a differential scanning calorimeter (DSC 2920, TA Instruments, New Castle, USA) previously calibrated with indium; an empty pan was used as reference. The temperature ranged from

30 to 120 °C at 10 °C/min. Gelatinized starches were stored at 4 °C for 7 d and heated again for analysis of retrogradation. The peak temperature of gelatinization (Tp), the enthalpy of gelatinization (ΔHg) and retrogradation (ΔHr), were obtained with the TA Universal Analysis 2000 program.

Starch swelling power

It was determined as described by Vega-Alvarez *et al.* (2022). About 40 mg of dry starch were mixed with 1 mL of deionized water, shaken vigorously and incubated for 30 min at 92.5 °C with gentle shaking by inversion. The sample was left to cool down to room temperature, centrifuged (17,000 *g*, 10 min) and the weight of the pellet was divided by the weight of the dry starch.

Branch-chain length distribution of amylopectin

The procedure described by Chávez-Murillo *et al.* (2012) was used. Starch (10 mg) was mixed with 3.2 mL of deionized water and boiled for 1 h. After cooling to room temperature, the sample was debranched by adding 0.4 mL of 0.1 mol/L sodium acetate (pH 3.5) and 5 µL of isoamylase (EC 3.2.1.68) (59 000 U/mg, Hayashibara Biochemical Laboratories, Japan) and the mixture incubated at 40 °C for 4 h. Debranched starch was analyzed with an ion-chromatography system equipped with a pulsed amperometric detector (DX-500, Dionex, Sunnyvale, CA, USA). A 10 µL aliquot was loaded into a CarboPac PA1 analytical column (4 × 250 mm, Dionex, Sunnyvale, CA, USA), and the separation was achieved with 0.15 mol/L NaOH (eluent A) and 0.15 mol/L NaOH/0.5 mol/L sodium acetate (eluent B) running at 5 mL/min. The A:B gradient was 95:5 % for 5 min, 60:40 % for 18 min, 15:85 % for 55 min and 95:5 % for 75 min. Data was analyzed with Chromeleon software 6.80 (Thermo Scientific, MA, USA). The chain-length distribution was determined as a percentage of the total peak area.

Activity of starch biosynthetic enzymes

ADP glucose pyrophosphorylase (AGPase)

The AGPase activity was determined according to Nishi *et al.* (2001) with some modifications. About 0.5 g of developing endosperm (28 DAP) was homogenized with 2 mL of cold extraction buffer [50 mmol/L HEPES-NaOH, pH 7.2, 2 mmol/L $MgCl_2$, 50 mmol/L 2-mercaptoetanol and 125 mL/L glycerol] and centrifuged (15,000 *g*, 15 min, 2 °C). The supernatant (crude enzyme extract) was mixed with 0.15 mL of a solution containing 100 mmol/L HEPES-NaOH, (pH 7.4), 3 mmol/L 3-phosphoglycerate, 1.2 mmol/L ADP-glucose, 3 mmol/L sodium pyrophosphate, 5 mmol/L $MgCl_2$, and 4 mmol/L dithiotreitol, and incubated for 20 min at 30 °C. The mixture was placed in boiling water for 2 min to inactivate the enzyme, then added with 350 µL of distilled water and centrifuged (15,000 *g*, 10 min, 2 °C). The supernatant (500 µL) was mixed with 0.15 mg $NADP^+$, 0.4 U phosphoglucomutase (Sigma, P3397) and 0.5 U glucose-6-phosphate dehydrogenase (Type XV, Sigma G6378), and incubated for 30 min at 30 °C. The enzyme activity was measured as the increase in absorbance at 340 nm and expressed as µmol of NAPDH produced per min (U) per g of sample on a fresh weight (fw) basis (U/g fw).

Granule bound starch synthase (GBSS)

The assay was conducted as described by Lee *et al.* (2014) with some modifications. About 0.5 g of developing endosperm was homogenized with 2 mL of cold extraction buffer (100 mmol/L Tris-HCl, pH 7.2, 2 mmol/L EDTA, 2 mmol/L DTT, 100 mL/L ethanediol), centrifuged (15,500 *g*, 30 min, 2 °C) and the pellet washed three times with cold extraction buffer. The pellet was resuspended in 3 mL of extraction buffer; then, 0.15 mL were mixed with 0.15 mL of solution A (50 mmol/L HEPES-NaOH, pH 7.4, 1.6 mmol/L ADP glucose, 0.7 mg amylopectin, 15 mmol/L DTT) and incubated at 30 °C for 1 h. The mixture was placed in boiling water for 30 - 40 s to inactivate the enzyme and then left on ice for 10 min. It was added with 0.1 mL of solution B (50 mmol/L HEPES-NaOH, pH 7.4, 10 mm/L phosphocreatine, 200 mmol/L KCl, 10 mmol/L $MgCl_2$, 5 U creatine phosphokinase (Type I)) and incubated at 30 °C for 30 min. The ADP produced by the starch synthase reaction was converted to ATP and the resulting solution was heated in boiling water for 30 s, then incubated on ice for 10 min, and centrifuged (17,000 *g*, 25 min, 2 °C). A 0.3 mL aliquot of the supernatant was mixed with 0.3 mL of solution C (50 mmol/L HEPES-NaOH, pH 7.4, 10 mmol/L glucose, 20 mmol/L $MgCl_2$, 2 mmol/L $NADP^+$). The activity of GBSSI was measured as the increase in absorbance at 340 nm after the addition of 1.4 U of hexokinase (*Sacharomyces cerevisiae*, Sigma H6380) and 0.35 U of glucose-6-phosphate dehydrogenase (Type XV, Sigma G6378) and incubation at 25 °C for 30 min. The results were expressed as U/g fw.

Starch branching enzyme (SBE)

The activity of SBE was estimated as described by Lee *et al.* (2014) with some modifications. About 0.5 g of developing endosperm (28 DAP) was macerated in 2 mL of cold extraction buffer (50 mmol/L HEPES-NaOH, pH 7.4, 4 mmol/L $MgCl_2$, 50 mmol/L 2-mercaptoethanol, 125 mL/L glycerol) and the mixture was centrifuged at 17,000 *g* for 25 min. The supernatant was passed through a filter paper (0.45 µm, Whatman) and the filtrate was used as the enzyme extract. SBE activity was assayed monitoring the stimulation of α-glucan synthesis from glucose-1-phosphate by rabbit muscle phosphorylase. A 100-µL aliquot of the enzyme extract was mixed with 100 µL of cold reaction buffer [50 mmol/L HEPES-NaOH, pH 7.0, 50 mmol/L glucose-1-phosphate, 2.5 mmol/L AMP, 1.2 U of phosphorylase a from rabbit muscle (Sigma P1261)], and incubated at 30 °C for 30 min. The reaction was ended by adding 50 µL of 1 mol/L HCl, and then mixed with 500 µL of DMSO. The solution was added with 700 µL of fresh iodine-potassium iodide solution (120 mmol/L KI, 8 mmol/L I2) and then incubated for 30 min at 30 °C in darkness. The SBE activity was determined by measuring the absorbance at 540 nm and the results were expressed as U/g fw.

Pullulanase activity assay (PULL)

The activity of PUL was determined according to Wu *et al.* (2015) with some modifications. Developing endosperms (28 DAP) were ground to a fine powder in liquid nitrogen. For

each mg of fine powder, 2 µL of cold extraction buffer (50 mmol/L Tris-Acetate pH 8.0, 10 mmol/L EDTA, 5 mmol/L DTT) were added and mixed for 2 min. The mixture was centrifuged (16,000 *g*, 10 min, 4 °C) and the supernatant used as the enzyme extract. Red-pullulan (Megazyme, Wicklow, Ireland) was used to measure the activity of pullulanase following the manufacturer´s instructions. The results were expressed as U/g fw.

Full length *Ae1* cDNA sequencing and sequence alignment

The full cDNA sequence of *Ae1* from the maize line B73 (http://www.maizegdb.org/) was used to design five pairs of primers (Table 1) with the Primer-BLAST program (http://www.ncbi.nlm.nih.gov/tools/primer-blast/). Total RNA was extracted from developing endosperms (28 DAP) of K0326Y-QPM and W64A*o2* as described previously (Vega-Alvarez *et al.*, 2022). The cDNAs were obtained with the kit SCRIPT cDNA Synthesis (Jena Bioscience) and 50 ng were used for PCR reactions The amplification was performed in a C1000 touch thermocycler (Bio-Rad, CA, USA) programmed with the following conditions: denaturation at 95 °C for 5 min, followed by 30 cycles of 1 min at 94 °C (denaturation), 1 min at X °C (alignment) (Table 1) and 1 min at 72 °C (extension), with a final extension period of 5 min at 72 °C. The amplified fragments were separated in 1% agarose gels, purified using the UltraClean 15 DNA Purification kit (MO BIO, California, USA) and sequenced at the Institute of Biotechnology of the National Autonomous University of Mexico. SnapGene version 5.0.7 was used to assemble the sequence of the fragments using as reference the B73 sequence (MaizeGDB Gene ID GRMZM2G032628_T01), and to perform the alignment of the sequences obtained for the parental lines. The cDNA sequences of K0326Y-QPM and W64A*o2* were submitted to GenBank with the accession numbers ON637850 and OQ030199, respectively.

Production and activity of recombinant SBEIIb

The *Ae1* cDNA sequences of K032Y-QPM and W64A*o2* were synthesized and cloned into the vector pET-29a(+) by ProteoGenix (https://www.proteogenix.science/). They were used to transform *E. coli* BL21 cells by the heat-shock method (Deshmukh *et al.*, 2022). Plasmid DNA was extracted to confirm the correct insertion of the *Ae1* gene by restriction analysis with BgtI. The expression of pET-29a(+) in *E. coli* was induced with 1 mmol/L of IPTG. Recombinant SBEIIb was partially purified from inclusion bodies, solubilized in 5 mol/L guanidine hydrochloride, and purified by affinity chromatography using a HiTrapTM chelating column HP (GE Healthcare, Chicago, IL, USA). Proteins were separated by SDS-PAGE and transferred to a nitrocellulose membrane (Hybond™-ECL™ Amersham Bioscience). The membrane was blocked with 5 % non-fat milk (Svelty, Nestle®) and incubated with a 6X His tag antibody (Sigma), followed by HRP-conjugated goat anti-rabbit IgG (Sigma) as secondary antibody. The activity of the recombinant enzymes was determined as described previously for endosperm using 80 µg of protein extract (Lee *et al.*, 2014).

Statistical analysis

A completely randomized design with three replications was used. A one-way ANOVA was performed combined with the Fisher test ($p \leq 0.05$) for mean comparisons. The independent variable was the maize line and the response variables were starch composition and thermal properties, amylopectin branch-chain length distribution and enzymatic activities. The *t* test was used to compare the average length of the amylopectin branches between the vitreous and opaque lines. All analyses were performed using the software STATGRAPHICS centurion version 5.1 (Statistical Graphics Corporation™, Maryland, USA).

RESULTS AND DISCUSSION

Starch physicochemical properties

The composition and thermal properties of starch was evaluated in developing endosperm (28 DAP) from K0326Y-QPM, W64A*o2* and six RILs contrasting in vitreousness (Table 2). Total starch content was not significantly different between the parental lines, but the opaque RILs showed higher

Table 2. Composition and thermal properties of starch from developing endosperm of maize lines contrasting in vitreousness.
Tabla 2. Composición y propiedades térmicas de almidón de endospermo en desarrollo de líneas de maíz contrastantes en vitrosidad.

Maize Line[1]	Total starch (g/100 g flour)	Amylose (g/100 g starch)	Amylopectin (g/100 g starch)	SP[2] (g/g starch)	ΔHg[3] (J/g)	Tp[4] (°C)	R[5] (%)
K0326Y-QPM (V)	52.2 ± 0.3^{bc}	20.6 ± 0.4^{bc}	79.4 ± 0.4^{cd}	13.6 ± 0.4^{c}	9.7 ± 0.4^{d}	70.6 ± 0.2^{ab}	46.3 ± 3.9^{b}
W64A*o2* (O)	52.8 ± 0.4^{ab}	18.3 ± 0.4^{d}	81.7 ± 0.4^{b}	14.7 ± 0.5^{ab}	12.3 ± 0.3^{a}	69.9 ± 0.2^{c}	33.4 ± 2.1^{c}
21 (V)	50.8 ± 0.2^{e}	22.4 ± 0.3^{a}	77.6 ± 0.3^{e}	13.5 ± 0.2^{cd}	6.5 ± 0.2^{f}	69.9 ± 0.1^{c}	59.9 ± 1.3^{a}
305 (V)	51.5 ± 0.2^{cd}	21.1 ± 0.7^{b}	78.9 ± 0.7^{d}	12.9 ± 0.4^{de}	6.9 ± 0.2^{f}	70.8 ± 0.4^{a}	45.3 ± 0.6^{b}
346 (V)	51.3 ± 0.5^{de}	19.7 ± 0.6^{c}	80.3 ± 0.6^{c}	12.5 ± 0.2^{e}	7.9 ± 0.5^{e}	69.5 ± 0.1^{d}	46.5 ± 0.9^{b}
55 (O)	52.6 ± 0.4^{ab}	16.2 ± 0.9^{e}	83.4 ± 0.9^{a}	14.7 ± 0.3^{b}	11.3 ± 0.2^{b}	69.9 ± 0.1^{c}	33.6 ± 1.1^{c}
73 (O)	53.0 ± 0.9^{a}	16.5 ± 0.4^{e}	83.5 ± 0.4^{a}	15.3 ± 0.3^{a}	10.9 ± 0.5^{bc}	69.9 ± 0.5^{c}	32.3 ± 4.2^{c}
123 (O)	52.9 ± 0.3^{ab}	16.9 ± 0.5^{e}	83.1 ± 0.5^{a}	15.2 ± 0.6^{ab}	10.6 ± 0.2^{c}	70.3 ± 0.1^{b}	30.3 ± 3.1^{c}

[1]V: Vitreous sample with the genotype corresponding to K0326Y-QPM; O: Opaque sample with the genotype corresponding to W64A*o2*; [2]Swelling power; [3]Gelatinization enthalpy; [4]Peak gelatinization temperature; [5]Percent retrogradation. Different superscript letters in the same column indicate significant differences based on the Fisher test ($P \leq 0.05$).
[1]V: Muestra vítrea con el genotipo correspondiente a K0326Y-QPM; O: Muestra opaca con el genotipo correspondiente a W64A*o2*; [2]Poder de hinchamiento; [3]Entalpía de gelatinización; [4]Temperatura pico de gelatinización; [5]Porcentaje de retrogradación. Letras superíndice diferentes en la misma columna indican diferencias significativas de acuerdo con la prueba de Fisher ($P \leq 0.05$).

values than the vitreous lines. The amylose/amylopectin ratio has an important effect on the starch physicochemical, structural and functional properties. For example, starch with high amylopectin content has high viscosity and digestibility, whereas a high proportion of amylose is associated with more resistant starch after thermal processing and less digestibility, which may be useful to reduce glycemic levels and for other industrial applications (Varghese *et al.*, 2023). The starch of the vitreous lines showed greater content of amylose compared to their opaque counterparts (Table 2). This behavior was previously observed in mature endosperm of QPM lines, and the higher proportion of amylose was associated with less crystalline starch and more compact granules with angular shapes (Salazar-Salas *et al.*, 2014). Another study also reported a higher amylose content and less crystalline starch in the vitreous endosperm of mature kernels from five normal maize inbred lines (Xu *et al.*, 2019), indicating an important role for amylose in the formation of the vitreous phenotype.

The analysis of starch thermal properties showed a narrow range for peak gelatinization temperatures (Tp, 69.5-70.6 °C), while the gelatinization enthalpy (ΔHg) was significantly higher in the opaque than in the vitreous lines (Table 2). Gelatinization involves the dissociation of the double helices that form the crystalline structure of amylopectin in the presence of excess water, which explains the higher energy registered in lines with greater amylopectin content (Table 2) and the positive correlation observed between these properties (r = 0.81, $P \leq 0.001$). Similar results were reported by Salazar-Salas *et al.* (2014) and Wu *et al.* (2015). Retrogradation occurs when gelatinized starches reassociate to form ordered structures. The percent retrogradation (R) values were higher in the vitreous than in the opaque lines (Table 2), showing a positive correlation with the amylose content (r = 0.89, $P \leq 0.001$). Previous studies have suggested that amylose is the main component responsible for the short-term retrogradation where the linear chains interact through hydrogen bonds, forming a mesh that grows or thickens as the storage time elapses (Chung and Liu, 2009). Swelling power (SP), which indicates the water holding capacity of gelatinized starch, were higher in the opaque than in the vitreous lines (Table 2) and correlated negatively with the amylose content (r = - 0.738, $P \leq 0.001$). The asymmetric distribution of amylopectin in the starch granules favors the entry of water, whereas amylose acts as a diluent or it may form complexes with lipids that prevent swelling (Zhao *et al.*, 2022).

Activity of starch biosynthetic enzymes

The biochemical basis of the variation in starch properties was studied by measuring the activity of starch biosynthetic enzymes in K0326Y QPM, W64A*o2* and six RILs contrasting in kernel vitreousness (Fig. 1). An advanced stage (28 DAP) of endosperm development was chosen because the enzyme activities and starch properties may show a better associa-

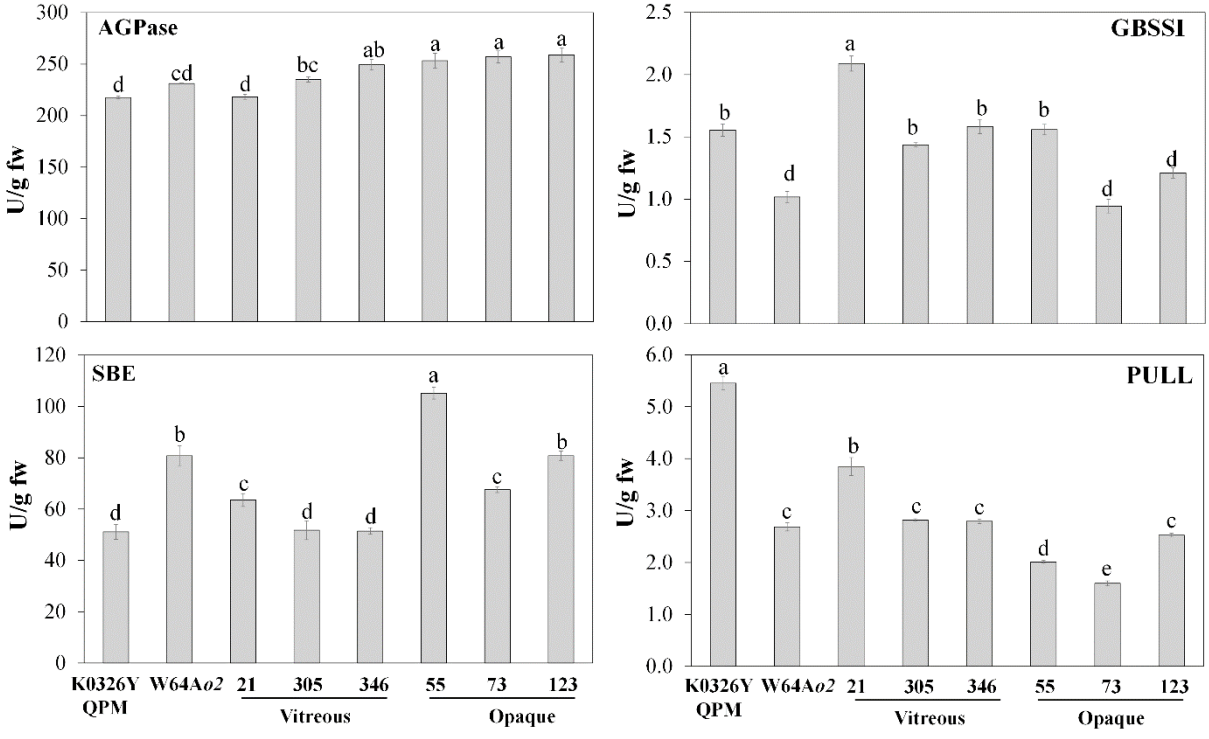

Figure 1. Activity of starch biosynthetic enzymes in developing endosperm (28 DAP) of maize lines contrasting in vitreousness. AGPase, ADP-glucose pyrophosphorylase; GBSS, Granule-bound starch synthase; SBE, Starch branching enzyme; PULL, Pullulanase. Different letters indicate significant differences based on the Fisher test ($P \leq 0.05$).

Figura 1. Actividad de enzimas de síntesis de almidón en endospermo en desarrollo (28 DAP) de líneas de maíz contrastantes en vitrosidad. AGPase, ADP-glucosa pirofosforilasa; GBSS, Almidón sintasa unida al gránulo; SBE, Enzima ramificadora de almidón; PULL, Pullulanasa. Letras diferentes indican diferencias significativas de acuerdo con la prueba de Fisher ($P \leq 0.05$).

tion with the vitreous phenotype in mature endosperm. ADP-glucose pyrophosphorylase (AGPase) is a key regulatory enzyme in starch biosynthesis. It catalyzes the rate-limiting step that produces ADP-glucose from glucose 1-phosphate and ATP. The activity of this enzyme was not significantly different between W64A*o2* and K0326Y-QPM, although the opaque RILs in general showed higher activity values than the vitreous lines (Fig. 1). These results correspond with the higher starch content observed in the opaque lines (Table 2) and the positive correlation reported between AGPase activity and starch content (Zhang *et al.*, 2008).

GBSS is responsible for amylose biosynthesis and is tightly bound to starch granules where it catalyzes the formation of α-1,4 linkages between glucose residues and glucan substrates. The parental K0326Y-QPM and the vitreous RILs lines showed in general higher GBSS activity compared to the opaque lines (Fig. 1), agreeing with the higher expression levels of the gene encoding this enzyme (*Wx1*) reported in vitreous lines (Vega-Alvarez *et al.*, 2022). GBSS activity also showed a positive correlation with amylose content (r= 0.678, $P \leq 0.001$) as previously reported by Zhang *et al.* (2008). Thus, the higher GBSS activity during endosperm development in the vitreous QPM lines contributes to the synthesis of starch granules with a greater proportion of amylose and amorphous regions that may favor their compaction and interaction with protein bodies, resulting in the vitreous phenotype of the mature endosperm (Salazar-Salas *et al.*, 2014).

The SBE is responsible for the formation of α-1,6-branch points during amylopectin biosynthesis. The parental line W64A*o2* and the opaque RILs showed higher SBE activity than the vitreous lines (Fig. 1), which is coincident with the positive correlation observed between the activity of this enzyme and the amylopectin content (r = 0.683, $P = 0.001$). The main SBE isoform in maize endosperm is SBEIIb and its deficiency reduces the synthesis of starch, which contains higher amylose content and amylopectin with long internal chain lengths and less proportion of short branches, leading to elongated and smaller starch granules associated with enhanced resistance to gelatinization and hydrolysis (Zhong *et al.*, 2020; Han *et al.*, 2022). The amylopectin branch-length distribution of the maize lines contrasting in vitreousness is shown in Table 3. The parental lines, K0326Y QPM and W64A*o2* did not show significant differences, but in general the starches from the opaque lines showed the highest proportion of short chains (A chain: DP 6-12) and a positive correlation with SBE activity (r = 0.407, $P \leq 0.05$), while the proportion of B chains (DP 13-24) was higher in most of the vitreous lines, showing a positive association with amylose content (r = 0.781, $P \leq 0.001$) and the opposite with gelatinization enthalpy (r= -0.491, $P \leq 0.01$). These results correspond with previous studies indicating a greater proportion of B chains in starch samples from mature endosperm of vitreous lines, which also showed less crystallinity (Salazar-Salas *et al.*, 2014). It has been reported that SBEIIb form complexes with the soluble starch synthases SSI and SSIIa that modulate the fine structure of amylopectin by the assembly of small to intermediate sized clusters (Liu *et al.*, 2009), therefore the greater proportion of amylopectin B chains in the vitreous lines could be a compensatory effect of these starch synthases. Thus, SBEIIb may also play an important role in the formation of the vitreous endosperm considering that a reduction in the activity of this enzyme favors the synthesis of starch with higher amylose content and less crystallinity, which facilitates the compaction of the starch granules.

In the case of pullulanase, higher activity was observed in the vitreous lines compared to the opaque lines (Fig. 1), which corresponded with the positive correlation between the activity of this enzyme and vitreousness (r = 0.613, $P \leq 0.05$) reported by Wu *et al.* (2015). These authors proposed that pullulanase activity is affected by SSIII and together influence the kernel vitrousness by altering the fine structure of amylopectin.

Table 3. Amylopectin branch-chain length distribution of starches from developing endosperm of maize lines contrasting in vitreousness.

Tabla 3. Distribución de la longitud de las ramificaciones de amilopectina de almidones de endospermo en desarrollo de líneas de maíz contrastrantes en vitrosidad.

Maize Line	DP (6-12)	DP (13-24)	DP (25-36)	DP≥37	CL
K0326Y-QPM (V)	25.15^{d}	52.13^{a}	15.39^{ab}	7.33^{a}	19.30
21 (V)	25.51^{d}	52.05^{a}	15.49^{ab}	6.18^{b}	19.15
305 (V)	27.80^{c}	52.18^{a}	13.91^{c}	6.14^{b}	18.62
346 (V)	28.70^{bc}	50.14^{bc}	14.94^{bc}	6.26^{b}	18.69
Average Vitreous	**26.78**^{B}	**51.62**^{A}	**14.93**^{A}	**6.47**^{A}	**18.94**
W64A*o2* (O)	25.36^{d}	51.06^{ab}	16.27^{a}	7.30^{a}	19.50
55 (O)	30.90^{a}	48.87^{c}	13.89^{c}	6.32^{b}	18.45
73 (O)	30.00^{ab}	48.92^{c}	13.90^{c}	7.17^{a}	18.68
123 (O)	29.67^{ab}	49.50^{bc}	14.14^{c}	6.68^{ab}	18.66
Average Opaques	**28.98** ^{A}	**49.59**^{B}	**14.55**^{A}	**6.87**^{A}	**18.80**

DP= degree of polymerization; CL= average chain length. Different lowercase letters in a column indicate significant differences between the maize lines ($P \leq 0.05$). Different uppercase letters between the average values of vitreous and opaque lines in the bottom row indicate significant differentes based on the *t*-test ($P \leq 0.05$).

DP= grado de polimerización; CL= longitud promedio de cadena. Letras minúsculas diferentes en una columna indican diferencias entre las líneas de maíz ($P \leq 0.05$). Letras mayúsculas diferentes entre los valores promedio de líneas vítreas y opacas en la última fila indican diferencias significativas de acuerdo con la prueba *t* ($P \leq 0.05$).

Sequencing, three-dimensional modelling and activity of recombinant SBEIIb

Sequence alignment of Ae1 alleles

Full length cDNA sequences for *Ae1* (2675 bp) from K0326Y-QPM and W64A*o2* were assembled from five overlapping RT-PCR fragments and corresponded to that of the B73 maize line (acc. AFW71659.1). Sequence alignment showed eight single nucleotide polymorphisms (SNPs; Fig. 2): 1137 (T≠A), 1138 (A≠T), 1530 (T≠A), 1531 (G≠A), 1534 (C≠A), 1535 (T≠A), 1551 (T≠G) and 1578 (T≠C). Five of these SNPs generated changes in the amino acid sequence of SBEIIb at positions 379 His→Gln, 380 Ser→Cys, 510 Phe→Leu, 511 Ala→Thr and 512 Leu→Asn (Fig. 3). These amino acids are close to those located in the active site of the enzyme, Asp397, His402, Arg445, Asp447, Glu502, His569 and Asp570 (Abad *et al.*, 2002), which were conserved in the two parental lines. Kuriki

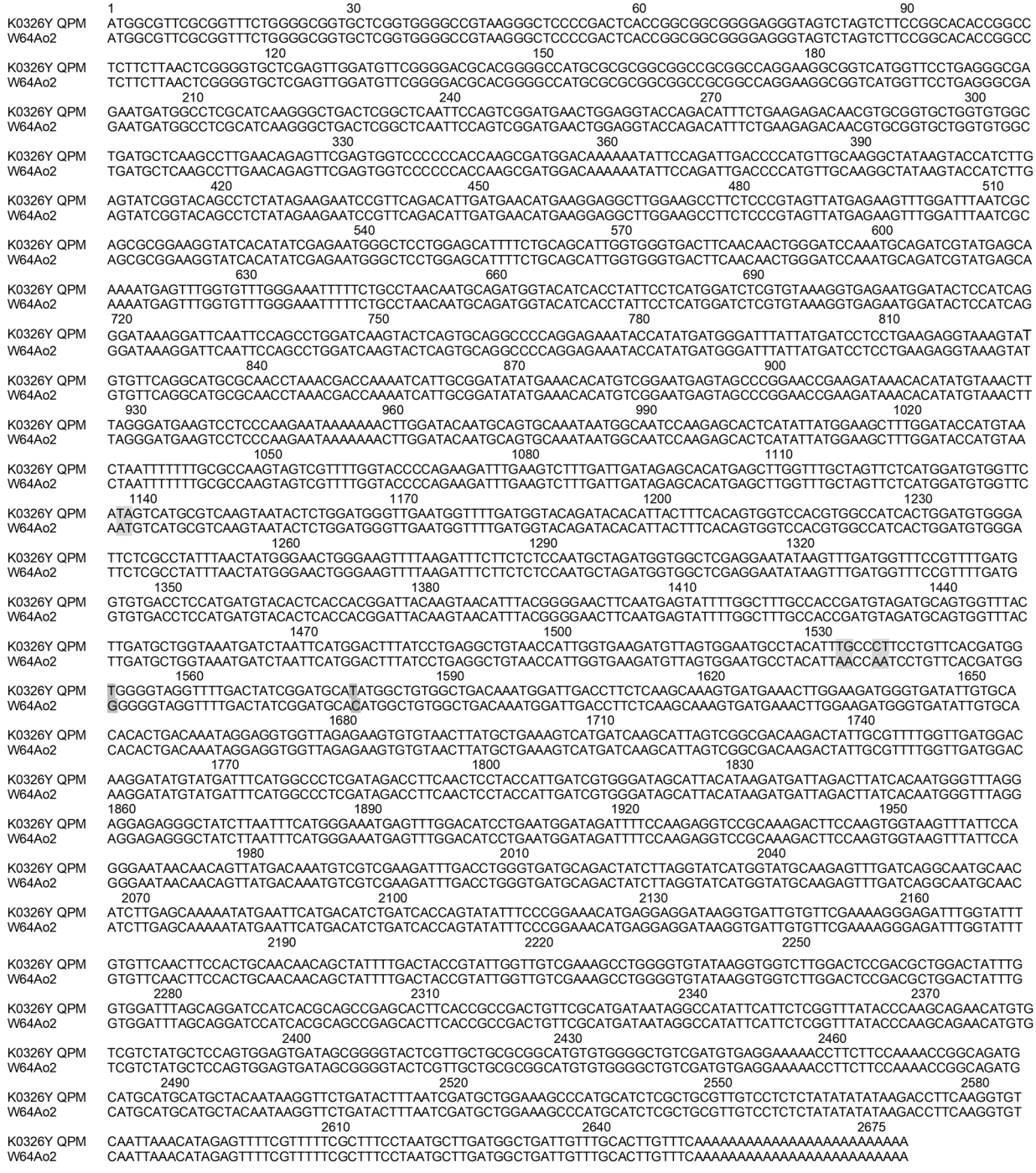

Figure 2. Multiple nucleotide sequence alignment of the *Ae1* coding region from K0326Y QPM and W64A*o2*. Nucleotide differences with grey background represent SNPs.

Figura 2. Alineamiento múltiple de secuencias nucleotídicas de la region codificante de Ae1 de K0326Y QPM and W64A*o2*. Las diferencias de nucléotidos con fondo gris representan SNPs.

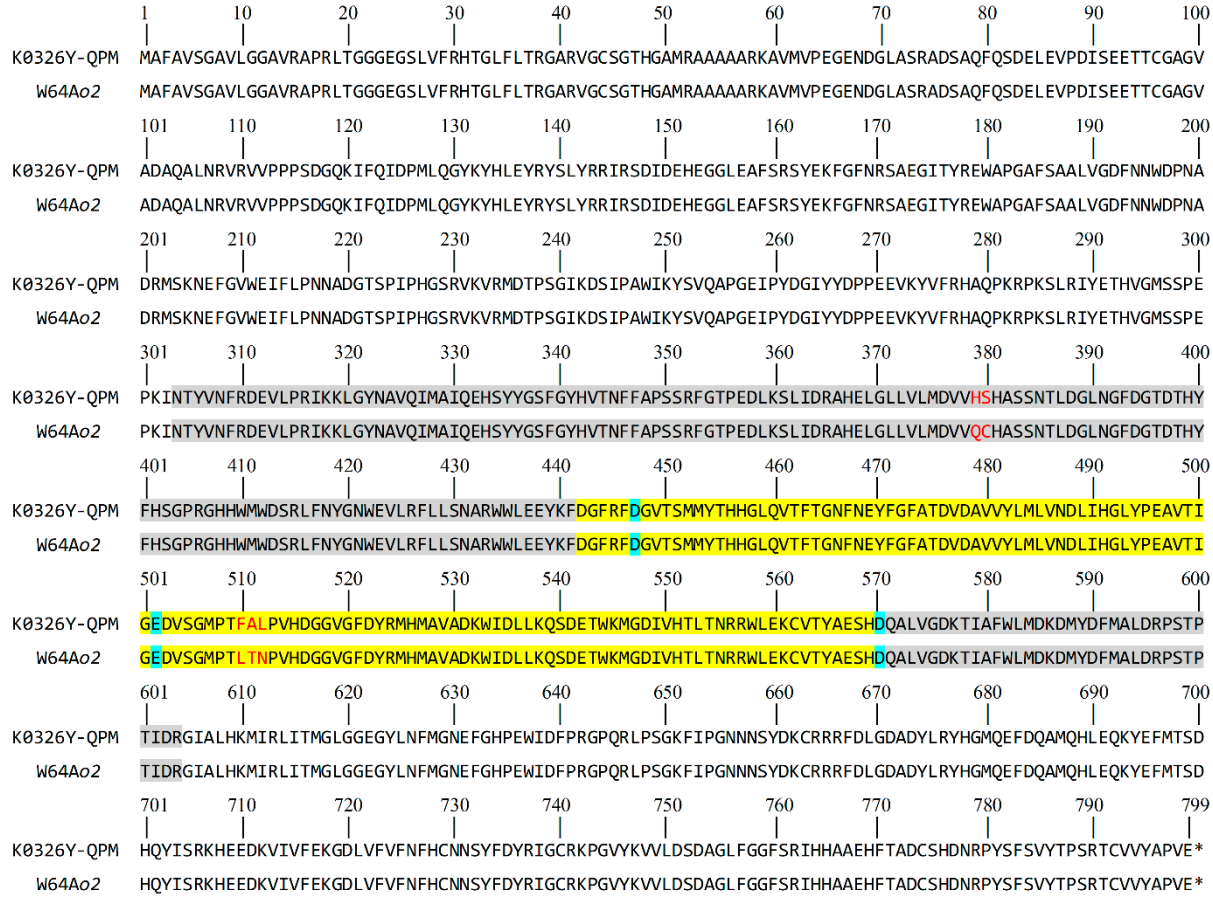

Figure 3. Alignment of starch branching enzyme translated amino acid sequences from K0326Y-QPM and W64A*o2*. The catalytic domain is highlighted in grey and the possible active site in yellow. The amino acid differences between the parental lines are indicated in red and the catalytic triad is highlighted in blue.
Figura 3. Alineamiento de las secuencias de aminoácidos traducidas de la enzima ramificadora de almidón de K0326Y-QPM y W64A*o2*. El dominio catalítico está resaltado en gris y el posible sitio activo en amarillo. Las diferencias de aminoácidos entre las líneas parentales se indican en rojo y la triada catalítica esta resaltada en azul.

et al. (1996) demonstrated by site-directed mutagenesis that the triad formed by Asp447, Glu502 and Asp570 is required for the catalytic activity of branching enzyme II from maize endosperm, while Funane *et al.* (1998) showed that two conserved histidine residues (His381 and His569) are critical for substrate binding. These amino acids were correctly identified in the present study (Fig. 3).

Three-dimensional modelling of SBEIIb

The comparison of the SBEIIb amino acid sequences from the parental lines showed five amino acid differences at positions close to the active site of the enzyme (Fig. 3). The prediction of the three-dimensional model using PHYRE2 (Kelley *et al.*, 2015) revealed that the amino acid changes at positions 510, 511 and 512 caused differences in the structure of the enzyme, affecting its catalytic site (Fig. 4). A greater opening between two alpha helices was observed in the active site of the opaque line W64A*o2* compared to the vitreous line K0326Y-QPM. It may be possible that the greater opening in the active site of SBEIIb facilitates the enzyme-substrate interaction, contributing to the higher activity observed in the opaque lines (Fig. 1).

Activity of recombinant SBEIIb

To determine if the activity of the SBEIIb enzymes in K0326Y-QPM and W64A*o2* vary because of their amino acid differences, *E. coli* BL21 cells were transformed with plasmids expressing the maize *Ae1*-K0326Y-QPM and *Ae1*-W64A*o2* sequences. SDS-PAGE (Fig. 5A) and immunoblotting (Fig. 5B) revealed the predicted 90.5 kDa band corresponding to the recombinant SBEIIb. These patterns are like those reported by other authors in maize (Liu *et al.*, 2009). The SBE activity of the purified protein extracts of the transformants *Ae1*-K0326Y QPM and *Ae1*-W64A*o2* did not show significant differences (Fig. 5C). This does not agree with the measurements determined from endosperm extracts (Fig. 1) and the predicted differences between the active sites (Fig. 4), which suggested that *Ae1*-W64A*o2* encodes an enzyme with higher activity. These discrepancies may be attributed to the fact that the SBE activity in maize endosperm is influenced by phosphorylation and the formation of heteromeric protein complexes with other starch biosynthetic enzymes (Liu *et al.*, 2009). Alternatively, the differences in activity observed in endosperm could be just due to the differences in the expression of the allelic variants as reported by Vega-Alvarez *et al.* (2022).

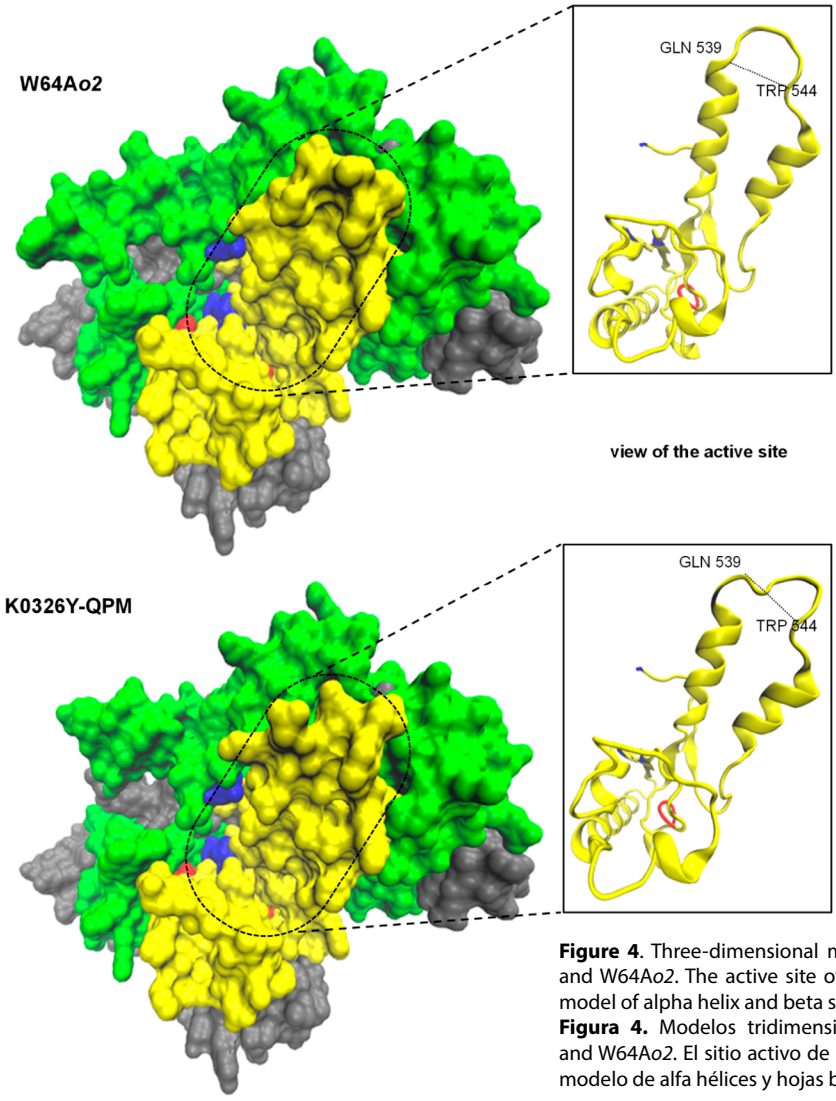

Figure 4. Three-dimensional models of SBEIIb from K0326Y-QPM and W64A*o2*. The active site of the enzyme is represented with a model of alpha helix and beta sheets.
Figura 4. Modelos tridimensionales de SBEIIb de K0326Y-QPM and W64A*o2*. El sitio activo de la enzima está representado con un modelo de alfa hélices y hojas beta.

Based on the predicted three-dimensional models of SBEIIb (Fig. 4), it was hypothesized that a greater opening in the active site may facilitate the enzyme-substrate interaction in W64A*o2*, resulting in higher activity. However, additional studies such as the use of an eukaryotic heterologous system and site-directed mutagenesis are required to confirm this hypothesis. This study provides additional information about the mechanisms associated with endosperm modification in QPM. The activity of starch biosynthetic enzymes in developing endosperm of vitreous genotypes was associated with the synthesis of starch granules with a higher amylose content and less cristallinity, which may favor their compaction and interaction with protein bodies and other cellular components after the disruption of the amyloplast membrane during kernel desiccation. This complements the mechanism associated with an increased number of small protein bodies rich in 27 kDa γ-zein that fill the spaces between starch granules (Wu *et al.*, 2010). The interaction between starch granules and protein bodies is very important not only for the vitreous phenotype but also for the improved nutritional value of QPM. The lysine content is increased by reducing the sythesis of α-zeins and by increasing the content of lysine-containing proteins that can be associated to the cytoskeleton that surrounds the protein bodies. This proteome rebalancing includes proteins involved in processes of starch and sucrose metabolism, amino acid biosynthesis, and protein processing in the endoplasmic reticulum, most of which are enriched in lysine, tryptophan and methionine, and therefore are responsible for the improved nutritional value (Zhao *et al.*, 2023).

The International Maize and Wheat Improvement Center (CIMMYT) has released hundreds of QPM genotypes, and this effort is being replicated by other breeding programs around the world (Maqbool *et al.*, 2021). However, breeding QPM is challenging because it requires the introduction of multiple *o2* modifier genes into an agronomical adapted *o2* genotype while maintaining the high nutritional value. Molecular markers linked to kernel hardness and amino acid content are available or being discovered, which represents a cost-effective tool to develop QPM genotypes. In this study

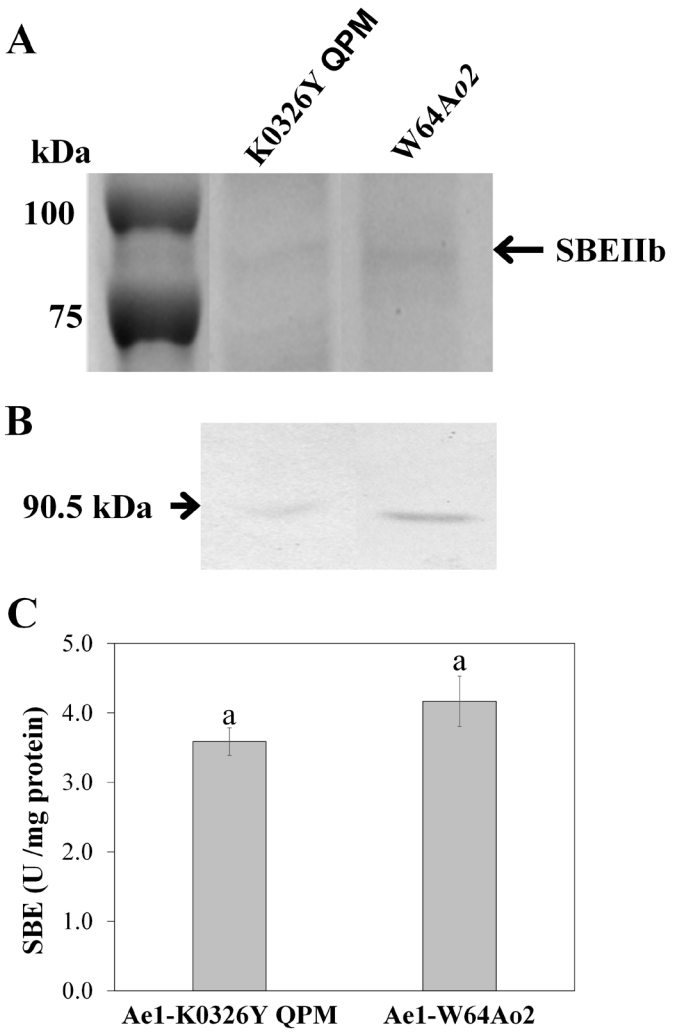

Figure 5. Expression and activity of recombinant SBEIIb from K0326Y QPM and W64A*o2*. (A) SDS-PAGE of affinity purified protein extract from *E. coli*. The band corresponding to SBEIIb is indicated on the right. (B) Immunoblot analysis of recombinant SBEIIb with anti-His antibodies. The molecular mass (kDa) of the recombinant protein is indicated on the left. (C) Specific activity of the recombinant SBEIIb of *Ae1*-K0326Y-QPM and *Ae1*-W64A*o2*. Different letters indicate significant differences based on the Fisher test ($P \leq 0.05$).

Figura 5. Expresión y actividad de SBEIIb recombinante de K0326Y QPM y W64A*o2*. (A) SDS-PAGE de extracto proteico de *E. coli* purificado por afinidad. La banda correspondiente a SBEIIb se indica a la derecha. (B) Analisis inmunológico de SBEIIb recombinante con anticuerpos anti-His. La masa molecular (kDa) de la proteína recombinante se indica a la izquierda. (C) Actividad específica de SBEIIb recombinante de *Ae1*-K0326Y-QPM y *Ae1*-W64A*o2*. Letras diferentes indican diferencias significativas de acuerdo con la prueba de Fisher ($P \leq 0.05$).

we also investigated if the differences in the sequence of the gene encoding the starch branching enzyme IIb may be used as a potential molecular marker, but additional studies are required to establish this association.

CONCLUSIONS

The vitreous phenotype in QPM is associated with modifications in the expression and activity of starch biosynthetic enzymes during endosperm development, that change the starch composition, physicochemical and structural properties. The increased activity of GBSSI and the reduced activity of SBE, produce starch granules with more amylose and less crystalline amylopectin, which may be favoring a greater compaction between these structures. The vitreous endosperm in maize has economic and agronomic importance. Vitreous kernels are less fragile and more adequate for market and storage. They are also more suitable to process some products such as grits, corn chips and corn flakes. Developing QPM genotypes has also great potential to improve human nutrition in developing countries where maize is a staple food.

ACKNOWLEDGMENTS

This research was funded by Consejo Nacional de Humanidades, Ciencia y Tecnología (CONAHCYT)-México, grant number 284552, and Universidad Autónoma de Sinaloa, grant number PROFAPI2015/221. DGGN and JCGO acknowledge the scholarship received from CONAHCYT-México.

CONFLICTS OF INTEREST

The authors declare they have no conflict of interest.

REFERENCES

Abad, M.C., Binderup, K., Rios-Steiner, J., Arni, R.K., Preiss, J. and Geiger, J.H. 2002. The X-ray crystallographic structure of *Escherichia coli* branching enzyme. Journal of Biological Chemistry 277: 42164-42170.

Chávez-Murillo, C.E., Méndez-Montealvo, G., Wang, Y.-J. and Bello-Pérez, L.A. 2012. Starch of diverse Mexican rice cultivars: physicochemical, structural, and nutritional features. Starch - Stärke 64: 745-756.

Chung, H.-J. and Liu, Q. 2009. Impact of molecular structure of amylopectin and amylose on amylose chain association during cooling. Carbohydrate Polymers 77: 807-815.

Deshmukh, S., Kulkarni, R. and Bose, K. 2022. Transformation and protein expression. In: Textbook on Cloning, Expression and Purification of Recombinant Proteins. K. Bose (ed.), pp. 83-114. Springer Nature, Singapore.

FAOSTAT. 2024. Food and agriculture data. Food and Agriculture Organization of the United Nations. Rome, Italy: Food and Agriculture Organization of the United Nations. [Accessed 27 May 2024]. Available in http://faostat.fao.org.

Funane, K., Libessart, N., Stewart, D., Michishita, T. and Preiss, J. 1998. Analysis of essential histidine residues of maize branching enzymes by chemical modification and site-directed mutagenesis. Journal of Protein Chemistry 17: 579-590.

Gonzalez-Nuñez, D.G., Pineda-Hidalgo, K.V., Salazar-Salas, N.Y. and Lopez-Valenzuela, J.A. 2023. Mechanisms associated with endosperm modification in quality protein maize. Biotecnia XXV: 79-89.

Han, N., Li, W., Xie, C. and Fu, F. 2022. The effects of SBEIIb gene mutation on physicochemical properties of starch in maize. Theoretical and Experimental Plant Physiology 34: 381-393.

Holding, D.R., Hunter, B.G., Klingler, J.P., Wu, S., Guo, X., Gibbon, B.C., Wu, R., Schulze, J.M., Jung, R. and Larkins, B.A. 2011. Characterization of opaque2 modifier QTLs and candidate genes in recombinant inbred lines derived from the K0326Y quality protein maize inbred. Theoretical and Applied Genetics 122: 783-794.

ISO. 2020. Rice — Determination of amylose content — Part 1: Spectrophotometric method with a defatting procedure by methanol and with calibration solutions of potato amylose and waxy rice amylopectin (ISO 6647-1:2020). International Organization of Standards. https://www.iso.org/standard/73669.html.

Kelley, L.A., Mezulis, S., Yates, C.M., Wass, M.N. and Sternberg, M.J. 2015. The Phyre2 web portal for protein modeling, prediction and analysis. Nature Protocols 10: 845-858.

Kuriki, T., Guan, H., Sivak, M. and Preiss, J. 1996. Analysis of the active center of branching enzyme II from maize endosperm. Journal of Protein Chemistry 15: 305-313.

Lee, H.J., Jee, M.G., Kim, J., Nogoy, F.M.C., Niño, M.C., Yu, D.A., Kim, M.S., Sun, M., Kang, K.K., Nou, I. and Cho, Y.G. 2014. Modification of starch composition using RNAi targeting soluble starch synthase I in *Japonica* rice. Plant Breeding and Biotechnology 2: 301-312.

Li, C., Xiang, X., Huang, Y., Zhou, Y., An, D., Dong, J., Zhao, C., Liu, H., Li, Y., Wang, Q., Du, C., Messing, J., Larkins, B.A., Wu, Y. and Wang, W. 2020. Long-read sequencing reveals genomic structural variations that underlie creation of quality protein maize. Nature Communications 11: 17.

Liu, F., Makhmoudova, A., Lee, E.A., Wait, R., Emes, M.J. and Tetlow, I.J. 2009. The amylose extender mutant of maize conditions novel protein–protein interactions between starch biosynthetic enzymes in amyloplasts. Journal of Experimental Botany 60: 4423-4440.

Maqbool, M.A., Issa, A.B. and Khokhar, E.S. 2021. Quality protein maize (QPM): Importance, genetics, timeline of different events, breeding strategies and varietal adoption. Plant Breeding 140: 375-399.

Mertz, E.T., Bates, L.S. and Nelson, O.E. 1964. Mutant gene that changes protein composition and increases lysine content of maize endosperm. Science 145: 279-280.

Nishi, A., Nakamura, Y., Tanaka, N. and Satoh, H. 2001. Biochemical and genetic analysis of the effects of amylose-extender mutation in rice endosperm. Plant Physiology 127: 459-472.

Salazar-Salas, N.Y., Pineda-Hidalgo, K.V., Chavez-Ontiveros, J., Gutierrez-Dorado, R., Reyes-Moreno, C., Bello-Pérez, L.A., Larkins, B.A. and Lopez-Valenzuela, J.A. 2014. Biochemical characterization of QTLs associated with endosperm modification in quality protein maize. Journal of Cereal Science 60: 255-263.

Varghese, S., Awana, M., Mondal, D., Rubiya, M.H., Melethil, K., Singh, A., Krishnan, V. and Thomas, B. 2023. Amylose–Amylopectin Ratio. In: Handbook of Biopolymers. S. Thomas, A. AR, C. Jose Chirayil and B. Thomas (eds.), pp. 1305-1334. Springer Nature, Singapore.

Vega-Alvarez, E., Pineda-Hidalgo, K.V., Salazar-Salas, N.Y., Soto-López, O.A., Canizalez-Roman, V.A., Garzón-Tiznado, J.A., Gutierrez-Dorado, R. and Lopez-Valenzuela, J.A. 2022. Genetic and molecular analysis of starch physicochemical properties and its relationship with endosperm modification in quality protein maize. Biotecnia XXIV: 140-149.

Wu, H., Clay, K., Thompson, S.S., Hennen-Bierwagen, T.A., Andrews, B.J., Zechmann, B. and Gibbon, B.C. 2015. Pullulanase and starch synthase III are associated with formation of vitreous endosperm in quality protein maize. PloS One 10: e0130856.

Wu, Y., Holding, D.R. and Messing, J. 2010. γ-zeins are essential for endosperm modification in quality protein maize. Proceedings of the National Academy of Sciences of the United States of America 107: 12810-12815.

Xu, A., Lin, L., Guo, K., Liu, T., Yin, Z. and Wei, C. 2019. Physicochemical properties of starches from vitreous and floury endosperms from the same maize kernels. Food Chemistry 291: 149-156.

Zhang, J.J., Hu, Y.F. and Huang, Y.B. 2008. Relationship between activities of key enzymes involved in starch synthesis and accumulation in maize inbred lines during grain filling. Russian Journal of Plant Physiology 55: 249-255.

Zhao, H.-l., Qin, Y., Xiao, Z.-y., Sun, Q., Gong, D.-m. and Qiu, F.-z. 2023. Revealing the process of storage protein rebalancing in high quality protein maize by proteomic and transcriptomic. Journal of Integrative Agriculture 22: 1308-1323.

Zhao, T., Zhang, H., Chen, F., Tong, P., Cao, W. and Jiang, Y. 2022. Study on structural changes of starches with different amylose content during gelatinization process. Starch - Stärke 74: 2100269.

Zhong, Y., Liu, L., Qu, J., Li, S., Blennow, A., Seytahmetovna, S.A., Liu, X. and Guo, D. 2020. The relationship between the expression pattern of starch biosynthesis enzymes and molecular structure of high amylose maize starch. Carbohydrate Polymers 247: 116681.